

Optimal flip angle and signal shaping for single-shot volumetric DREAM B_1 mapping

Rüdiger Stemberg¹, Daniel Brenner¹, and Tony Stöcker^{1,2}

¹German Center for Neurodegenerative Diseases (DZNE), Bonn, Germany, ²Department of Physics and Astronomy, University of Bonn, Bonn, Germany

Target Audience: MR physicists and engineers with a particular interest in ultra-fast B_1 mapping and imaging and ultra-high fields.

Purpose: To investigate optimal flip angles (FAs) for the recently proposed volumetric DREAM¹ variant 3DREAM², which provides whole brain B_1 and B_0 maps within less than 3 seconds by using a single STEAM³ preparation prior to 3D k-space acquisition. A Cartesian spiral-out k_y - k_z -view-ordering (both phase encoded) restricted to an elliptical subset, which supports 2D parallel imaging (PI) and 2D partial Fourier, is as essential for high acquisition efficiency as are minimized echo spacings ($ESP \sim 2.3$ ms), facilitated by short rect excitation pulses². Typical echo train lengths, $N_{max}=300$ –1000, thus correspond to short acquisition times in the order of typical brain tissue T_1 . Free-induction-decay (FID) and particularly stimulated echo (STE) signal evolution strongly depends on the flip angles (FA) employed. Variable FA design may deliver constant and maximized STE signal for the given N_{max} ⁴. Such majorly small FAs are, however, rather SNR-inefficient for large N_{max} and lead to an unfavorable FID increase over time. Instead we propose to employ a unique FA throughout the entire echo train that counterbalances T_1 recovery and hence immediately leads to a constant FID signal shape, while STE signals undergo a predictable exponential decay. Here, the optimal flip angle is derived and customized image processing is discussed to yield accurate B_1 maps.

Methods: From the FID-steady-state equation follows:

$$\beta = \arccos\left(\frac{1}{E_1} - \frac{1-E_1}{M_z(0)E_1}\right), \quad (1)$$

where $M_z(0) = M_0 \cos^2 \alpha$ approximates the longitudinal magnetization following STEAM preparation ($M_0 = 1$ when starting in equilibrium) and $E_1 = e^{-ESP/T_1}$ accounts for relaxation and recovery. In contrast to the Ernst angle, which solves for the maximum FID-st-st. following a transient-state period, we have required here that the FIDs assume $FID(N) = FID(0) = M_z(0) \sin \beta$ throughout the echo train. As a consequence, Eq. 1 is defined only for $ESP < 2 \operatorname{arctanh}(M_z(0))T_1 \equiv ESP_{max}$, which is a safe assumption for typical 3DREAM ($ESP/ESP_{max} \sim 0.0003$). Since the STEs, in contrast to the FIDs, are not supported by recovering magnetization, using the FID-st-st. FA leads to a known exponential decay, $STE(N) = STE(0)e^{-N\lambda}$, where $STE(0) = 0.5 \sin^2 \alpha \sin \beta$ denotes the first STE signal and $\lambda \equiv -\ln(E_1 \cos \beta)$. The spiral-out view-ordering results in a growth of the k-space radius according to $|k_r| \approx k_{max}[N/N_{max}]^{1/2}$. Distribution of the STE decay in the k_y - k_z -plane accordingly approximates a 2D Gaussian filter,

$$f(N) = e^{-\lambda N} \rightarrow f(k_r) \approx e^{-\lambda N_{max}(|k_r|/k_{max})^2}. \quad (2)$$

This may be regarded beneficial, considering that (i) the mapped fields are expected to vary smoothly, and (ii) it suppresses pronounced Gibbs ringing at small matrix sizes. Since the filter function is known (for actual=nominal FA), it may optionally be applied a posteriori to the flat FID data so as to result in consistent resolution properties of the magnitude images, I_{STE} and I_{FID} . An FA map is then computed according to $\hat{\alpha} = \arctan([2 I_{STE}/I_{FID}]^{1/2})$.

SIMULATION: A realistic single-shot 3DREAM protocol ($\alpha = 60^\circ$, k_y - k_z -matrix: 24×64 , PI: 2×2 , $N_{max}=291$, $ESP=2.72$ ms, RF spoiling) was assumed for extended phase graph⁵ simulations with varying B_1 (scaling factor for α and β) to generate numerical phantom data ($T_1=1400$ ms, $T_2=80$ ms, smaller than field-of-view/2). A corresponding nominal FID-st-st. FA of $\beta = 6.2^\circ$ was utilized. Images were reconstructed ignoring PI and applying 8-fold symmetric zero-padding to visualize Gibbs ringing with and without employing the FID filter, $f(N)$, according to Eq. 2. Relative B_1 amplitude is varied according to $1 - 0.5 \cos(y)$ with one period over $2/3$ of the phantom and $B_1=1$ beyond.

EXPERIMENT: A single-shot whole-brain 3DREAM protocol ($\alpha = 60^\circ$, k_y - k_z -matrix: 40×58 , PI= 2×1 , PF= $6/8 \times 1$, $ESP=2.4$ ms, $N_{max}=1120$) was performed on one subject using a Siemens 7 Tesla research scanner equipped with a 32 channel receive head coil (Nova Medical). The extremely long echo train was expected to emphasize the effect of FID filtering. Assuming $T_1=1400$ ms corresponds to a FID-st-st. flip angle of $\beta \approx 6^\circ$. The approximate FID filter $f(k_r)$ according to Eq. 2 was applied post-hoc to the FID image.

Results: Fig. 1A shows simulated FID and STE signals vs. pulse number and vs. actual k-space radius. The latter confirms a Gaussian STE distribution in k-space. Fig. 1B top displays the STE image and the simulated B_1 variations. Fig. 1B middle displays the corresponding FID image without filtering and the resulting FA map (relative B_1 by dividing through $\alpha = 60^\circ$). Pronounced Gibbs ringing and distorted iso-FA-lines reflect resolution inconsistencies between FID and STE image. Fig. 1B bottom displays the filtered FID image and corresponding FA map. The latter exhibits no Gibbs ringing (even at sharp edges) and minimized iso-FA line distortions. Figure 2 demonstrates in vivo applicability of the proposed FID-st-st. FA and appropriate FID filtering at 7 Tesla even for extremely long echo train lengths and natural variation of T_1 and B_1 .

Discussion: Even though the proposed st-st. FA is computed for only one fixed T_1 and ideal $B_1=1$, good performance for varying B_1 (simulations) and for various T_1 (in vivo) has been demonstrated. An appreciated side effect of FID filtering is the suppression of "late" FID signals, which consist of an increasing fraction of fresh, unprepared magnetization. This can be expected to increase the accuracy of FA maps. Finally, note that for repeated scans with non-complete recovery (multi-channel B_1 mapping with short TR) a different st-st. FA is obtained by appropriately setting $M_0 < 1$, which scales $M_z(0)$ in Eq. 1.

Conclusion: The use of a unique FID-st-st. FA (independent of N_{max}) for single-shot 3DREAM has been proposed, which generates well behaving FID and STE signals. Knowledge of the STE evolution compared to the constant FID allows for according FID filtering and thus results in identical resolution properties in both images, which has been shown to improve FA maps. The discussed method is transferable to conventional, slice-selective DREAM [1], in which case longer ESPs will result in larger FID-st-st. FAs and linear-centric view-ordering will result in an exponential STE shaping in k-space.

References: [1] Nehrke et al. MRM 68, 2012; [2] Brenner et al. In Proc. ISMRM 22, 2014; [3] Frahm et al. JMR 64, 1985; [4] Frahm et al. JMR 65, 1985; [5] Hennig CMR 3, 1991

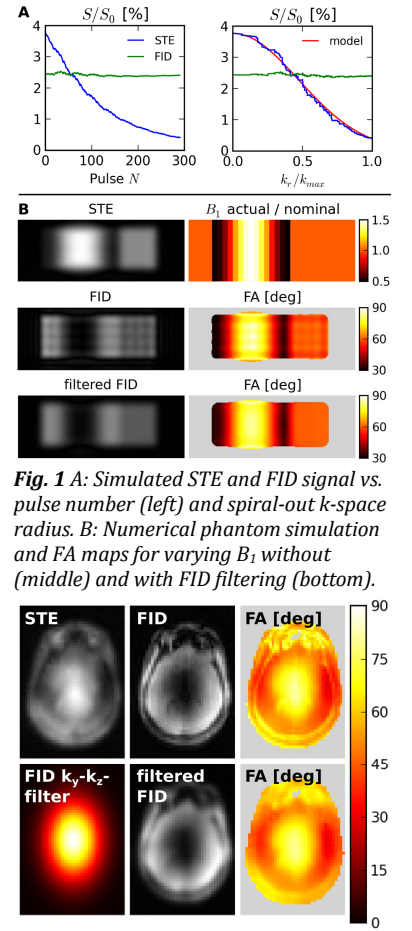


Fig. 1 A: Simulated STE and FID signal vs. pulse number (left) and spiral-out k-space radius. **B:** Numerical phantom simulation and FA maps for varying B_1 without (middle) and with FID filtering (bottom).

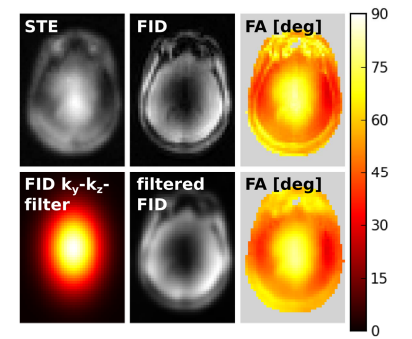


Fig. 2 In vivo 3DREAM with FID-st-st. FA=6° w/ and w/o FID filtering.